Chemistry & Biology
Article

Chemical Proteomics with Sulfonyl Fluoride Probes Reveals Selective Labeling of Functional Tyrosines in Glutathione Transferases

Christian Gu,[1] D. Alexander Shannon,[5] Tom Colby,[2] Zheming Wang,[1] Mohammed Shabab,[6] Selva Kumari,[1] Joji Grace Villamor,[1] Christopher J. McLaughlin,[5] Eranthie Weerapana,[3,5] Markus Kaiser,[4] Benjamin F. Cravatt,[3] and Renier A.L. van der Hoorn[1,*]
[1]The Plant Chemetics Laboratory
[2]Proteomics Service Center
Max Planck Institute for Plant Breeding Research, Carl-von-Linne Weg 10, 50829 Cologne, Germany
[3]Department of Chemical Physiology, The Scripps Research Institute, 10550 North Torrey Pines Road, La Jolla, CA 92037, USA
[4]Zentrum für Medizinische Biotechnologie, Fakultät für Biologie, Universität Duisburg-Essen, Universitätsstr. 2, 45117 Essen, Germany
[5]Department of Chemistry, Boston College, 2609 Beacon Street, Chestnut Hill, MA 02466, USA
[6]Department of Bioorganic Chemistry, Max Planck Institute for Chemical Ecology, Hans-Knöll-strasse 8, 07745 Jena, Germany
*Correspondence: hoorn@mpipz.mpg.de
http://dx.doi.org/10.1016/j.chembiol.2013.01.016

SUMMARY

Chemical probes have great potential for identifying functional residues in proteins in crude proteomes. Here we studied labeling sites of chemical probes based on sulfonyl fluorides (SFs) on plant and animal proteomes. Besides serine proteases and many other proteins, SF-based probes label Tyr residues in glutathione transferases (GSTs). The labeled GSTs represent four different GST classes that share less than 30% sequence identity. The targeted Tyr residues are located at similar positions in the promiscuous substrate binding site and are essential for GST function. The high selectivity of SF-based probes for functional Tyr residues in GSTs illustrates how these probes can be used for functional studies of GSTs and other proteins in crude proteomes.

INTRODUCTION

Technologies that describe new functional residues in proteins on a global rather than an individual basis are desperately needed to speed up the functional annotation of gene products generated by genome-sequencing projects. Chemical proteomics has been identified as a powerful tool in the area of functional annotation of protein functions (Jeffery and Bogyo, 2003; Rix and Superti-Furga, 2009). Chemical proteomics takes advantage of state-of-the-art mass spectrometry to identify labeled proteins and labeling sites for a diverse range of chemical probes. Depending on the nature of the probe, chemical proteomics thereby detects active sites and sites of posttranslational regulation in a broad range of proteins. Activity-based protein profiling (ABPP), for example, displays the availability and reactivity of active-site residues in diverse protein classes (Cravatt et al., 2008; Serim et al., 2012). Likewise, metabolic labeling of proteomes with chemical probes has revealed sites for posttranslational modifications such as acylation, glycosylation, and prenylation (Heal and Tate, 2010).

Recently, chemical proteomics has been expanded further by including reactivity probes, which carry only a reactive group (e.g., Weerapana et al., 2008). When used properly, reactivity probes globally identify hyperreactive amino acids in proteomes. Iodoacetamide probes, for example, preferentially react with hyperreactive Cys residues when used at low concentrations (Weerapana et al., 2010). Importantly, these hyperreactive residues are frequently found in active sites of proteins and at sites prone to posttranslational modification. Reactivity probes therefore inform us about known and previously unrecognized functional residues in proteins. To expand this application beyond cysteine residues, new chemical probes are needed to target other amino acids and facilitate the functional characterization of diverse proteins. Here, we introduce sulfonyl-fluoride (SF) probes to study hyperreactive residues in proteomes. SF probes based on the serine protease inhibitor 4-(2-aminoethyl) benzenesulfonylfluoride (AEBSF) have been used recently to detect labeling of various Ser proteases (Shannon et al., 2012; Yan et al., 2012). It was noted in these studies that many other proteins are labeled by SF probes. Here we show that SF-based probes target functionally important Tyr residues in glutathione transferases (GSTs).

GSTs are ubiquitous and abundant enzymes involved in detoxification and transport of endogenous and xenobiotic small molecules (Hayes et al., 2005). GSTs catalyze the conjugation of small-molecule electrophiles to glutathione and play a pivotal role in all kingdoms of life. Plant GSTs, for example, confer herbicide resistance and play roles in secondary metabolism and oxidative stress (Edwards et al., 2000; Dixon and Edwards, 2010). Likewise, pathogen GSTs are important in drug resistance. The helminth human pathogen *Schistosome japonica*, for example, uses *Sj*GST for detoxification of antischistosomal drugs (McTigue et al., 1995). Upregulation of human GSTs is associated with the development of resistance to, e.g., anticancer drugs (Townsend and Tew, 2003). Each organism produces dozens of GST proteins that represent at least five of the twelve different GST superfamilies (Sheehan et al., 2001).

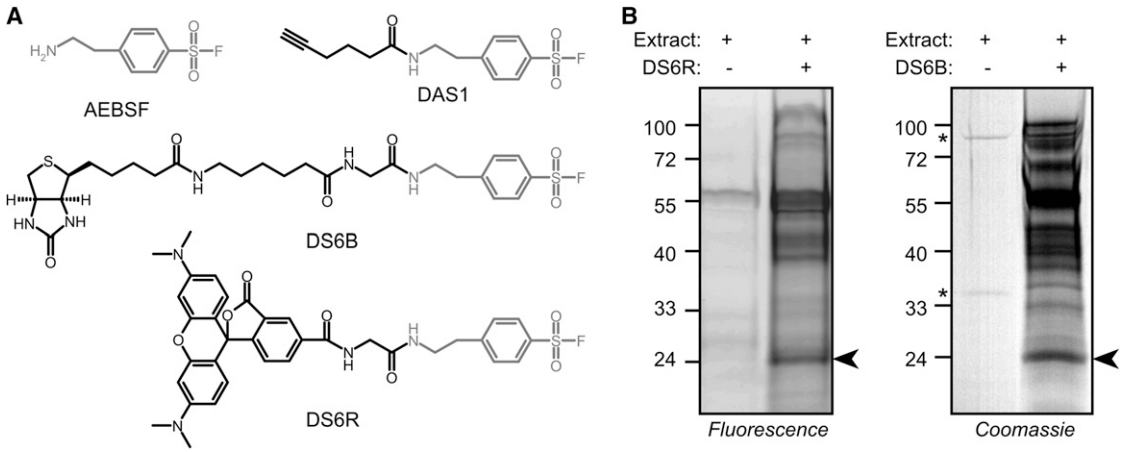

Figure 1. Structures and Labeling Characteristics of Sulfonyl Fluoride Probes

(A) Structures of the SF probes used in this study. The DS6B, DS6R, and DAS1 probes contain the AEBSF moiety (gray) with the reactive sulfonylfluoride (S–F). DS6B contains a biotin reporter tag, DS6R a fluorescent rhodamine reporter tag, and DAS1 an alkyne chemical handle for click chemistry.

(B) Labeling profiles of DS6R and DS6B are similar in *Arabidopsis* leaf proteomes. *Arabidopsis* leaf extract was labeled with and without DS6R or DS6B and either fluorescently labeled proteins were detected from protein gels using fluorescence scanning (left, DS6R), or biotinylated proteins were purified and detected on protein gels using Coomassie blue staining (right, DS6B). *, endogenously biotinylated proteins.

See also Figures S1 and S2.

Though structurally conserved, GSTs are highly diverse in protein sequence, and contain a promiscuous binding site (H-site) that can accommodate structurally diverse small molecules.

Despite the ubiquity and importance of GSTs in all kingdoms, chemical probes that monitor a large number of GSTs in proteomes have not yet been reported. Thus far, ABPP has monitored only omega-class GSTs, using probes that label the GST's catalytic cysteine (Weerapana et al., 2010). However, the catalytic Cys residue is not present in other GST families. Here, we discovered that GSTs of different families can be labeled by SF-based probes in different proteomes. Interestingly, these probes selectively label functionally important Tyr residues in the H-site. These probes open new avenues by which chemical proteomics can monitor the availability of hyperreactive residues of GSTs and other proteins in proteomes.

RESULTS

This study makes use of several AEBSF-based probes (Figure 1A). DS6B contains biotin, DS6R contains rhodamine, and DAS1 contains an alkyne, a chemical handle for click chemistry. These probes were initially aimed at detecting Ser proteases in proteomes, because AEBSF is a frequently used Ser protease inhibitor. When tested on *Arabidopsis* leaf proteomes, many labeled proteins were detected with both DS6R and DS6B, and the labeling profiles are comparable between the two probes (Figure 1B). Labeling was suppressed by adding an excess AEBSF, suggesting that the DS6R probes target the same residues as AEBSF (Figure S1A available online). Heat denaturation of the proteomes abolishes subsequent labeling, indicating that the protein folding is required for labeling (Figure S1B).

DS6B Labels Several Glutathione-S-Transferases

A hallmark signal at 24 kDa is consistently labeled and was further studied. Labeling of the 24 kDa signal occurs at neutral to basic pH (Figure S2). Mass spectroscopy (MS) analysis on purified DS6B-labeled proteins from *Arabidopsis* leaf extracts revealed that the 24 kDa signal contains at least three different glutathione-S-transferases (Table S1). *At*GSTU19 was identified by two unique peptides and *At*GSTU20 was identified by three unique peptides. *At*GSTF6 and *At*GSTF11 were identified by one peptide that is identical between these proteins. *At*GSTF6, *At*GSTF11, *At*GSTU19, and *At*GSTU20 have similar calculated molecular weights (MWs) of 23.5, 23.6, 25.7, and 25.0 kDa, respectively, consistent with the size of the DS6-labeled signal.

DS6B Labels Y208 in the C Terminus of *At*GSTU20

One of the *At*GSTU20 peptides contained a DS6B modification, which was included in the searches by allowing a modification of 579.22 Da (monoisotopic MW DS6B-HF) on any hydrophilic residue. The peptide from *At*GSTU20 with the sequence IVAYAAEYR has a mass of 1633.76, which is 579.2 Da bigger than expected for the unmodified peptide. The Mascot search engine failed to assign several peaks in the fragmentation spectrum, causing a relatively low mascot score for this labeled peptide. However, manual annotation of the peaks robustly identifies the DS6B labeling site (Figures 2 and S3). First, the fragmentation spectrum contains y ions of DS6B—biotin (B), linker-biotin (hB), and Gly-linker-biotin (GhB)—demonstrating that the DS6 modification is in the peptide. Second, the intense signal at 715.39 Da corresponds to an immonium ion of the DS6B-modified Tyr (Y*), indicating that DS6B is on one of the two tyrosines (IVAYAAEYR). Third, the b1–3 and y1–5 ion series, as well as the y5b6, y4b7, and y5b7 ions, have unmodified masses, indicating that the DS6B modification is not on the IVA or AAEYR sequences. This excludes the possibility that the second Tyr is modified and is in support of the first tyrosine being modified. Fourth, signals at 912.99, 884.98, and 956.08 Da correspond to internal y/b ions of the DS6B-modified peptides VAY*, AY*A/Y*AA, and AY*AA, respectively, demonstrating that the first Tyr is indeed

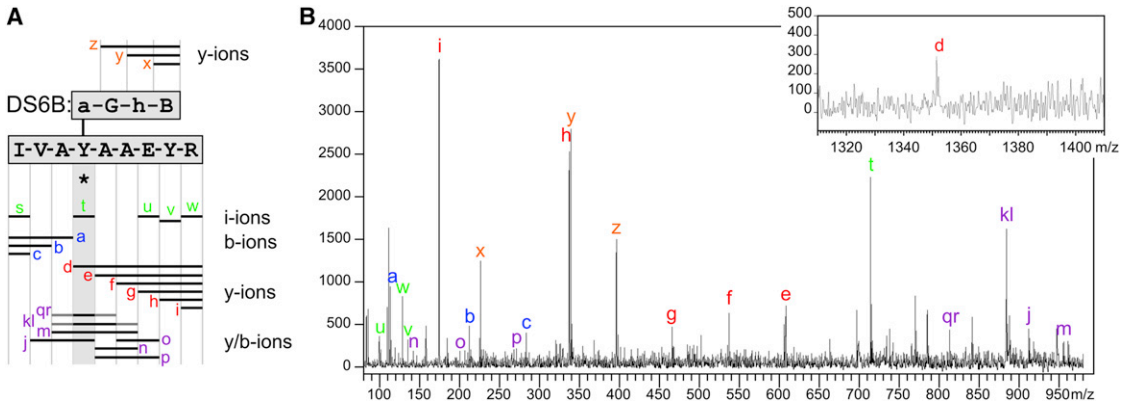

Figure 2. Peptide Fragmentation Spectrum Shows Labeling Site of DS6B in *At*GST20

(A) The *At*GST20 peptide IVAYAAEYR carries the DS6B modification on the first tyrosine. DS6B contains amide bonds that cause fragmentation into DS6B ions with biotin (B), the amin hexanoid acid linker (h), glycine (G), and AEBSF (a). The identified ions are indicated with bars above and below the DS6-modified sequence, as fragments from DS6B and the peptide, respectively. Peptides with an increased mass corresponding to the DS6B modification overlap with the gray bar indicated with an asterisk (*). The letters correspond to the peaks indicated in (B).

(B) Fragmentation spectrum of the DS6B-modified peptide. The letters correspond to the ions indicated in (A). The spectrum and its full assignment are shown in Figure S3.

See also Table S1.

labeled, because it is flanked by these residues. Fifth, a signal at 1,351.368 Da corresponds to the y6 ion, which includes the modified Tyr on the C-terminal fragment (Y*AAEYR). Taken together, these data demonstrate that the DS6B modification (*) is on the first Tyr of the peptide, IVAY*AAEYR, corresponding to Y208 in *At*GSTU20.

SF-Based Probes Target Various GSTs in Mouse Proteomes

In a similar series of parallel experiments, mouse liver and pancreas proteomes were labeled with DAS1, which contains a chemical alkyne handle that can be coupled to reporter tags using click chemistry. Labeling of mouse proteomes with DS6R produced a labeling profile that is distinct from that of plant proteomes but also contains a strong 25 kDa signal that is presumably caused by GSTs (Figure S4). Purification of DAS1-labeled proteins from mouse proteomes revealed an enrichment of ten different GSTs, including GSTA3, GSTA4, GSTK1, GSTM1–GSTM5, GSTO1, and GSTP1 (Table S2; Shannon et al., 2012).

To simultaneously identify the protein and its labeling site, DAS1 labeling sites were identified by tandem orthogonal proteolysis (TOP)-ABPP (Weerapana et al., 2007). Biotinylated peptides, generated by biotinylation of DAS1-labeled proteomes using click chemistry followed by whole-proteome trypsin digest, were purified. Modified peptides were eluted by TEV cleavage and analyzed by tandem MS (Weerapana et al., 2007). This experiment was performed several times on soluble proteomes of mouse liver and pancreas (Table S3). A total of 885 DAS1-modified peptide spectra were identified from the three GSTs (Table S4). Interestingly, the three identified GSTs represent three different classes: Mu (*Mm*GSTM1, 66 spectra), Omega (*Mm*GSTO1, 105 spectra), and Pi (*Mm*GSTP1, 392 spectra) (Table S4). These three classes are distinct from *At*GSTF6/7 and *At*GSTU19/20, which belong to the plant-specific Phi (F) and Tau (U) classes, respectively. Importantly, in all three mouse GSTs, the DAS1 modification was found on tyrosines: Y116 in *Mm*GSTM1, Y228 in *Mm*GSTO1, and Y108 in *Mm*GSTP1 (Table S4; sample spectra are shown in Figures S5A–S5C). These Tyr residues are not conserved in the primary amino acid sequence of the GSTs.

Labeling Occurs Consistently on Tyr Residues Located in the H-Site

The labeling sites on the four GSTs were mapped onto structural models of the GST proteins. The six structures available for mouse GSTP1 in the Protein Data Bank (PDB) differ in the ligands bound to the G-site but are similar in the conformation of the H-site. The structure of *Mm*GSTP1 bound to *p*-nitrobenzylglutathione (PDB ID code 1GSI; Vega et al., 1998) was chosen as a representative. Structural models for *At*GSTU20, *Mm*GSTM1, and *Mm*GSTO1 were generated using structures of Soybean GST Tau 4-4 (PDB ID code 3FHS; Axarli et al., 2009a), rat GSTM1 (PDB ID code 6GSV; Xiao et al., 1996), and human GSTO1-1 (PDB ID code 1EEM; Board et al., 2000), respectively, using SWISS MODEL (Arnold et al., 2006).

We generated an overlay of the four structural models to compare the labeling sites in GSTs. Despite the low sequence identity, the 3D structures of the different GSTs are sufficiently conserved to align the structures (Figure 3A). As expected, the glutathione binding site (G-site) is highly conserved between the various GSTs (Figure 3B). Importantly, despite the poor sequence conservation of the different GST protein sequences composing the H-site, the labeled Tyr residues from the Tau, Mu, Omega, and Pi classes cluster in the H-site, opposite to the G-site and consistently at 5.5–8.0 Å from the sulfur of the glutathione bound in the G-site (Figures 3B and S6). This consistency in location is particularly striking considering the fact that these Tyr residues are not conserved in the protein sequence and are positioned in the middle (Y116 in *Mm*GSTM1 and Y108 in *Mm*GSTP1) or in the C terminus (Y228 in *Mm*GSTO1 and Y206 in *At*GSTU20) of the GST proteins.

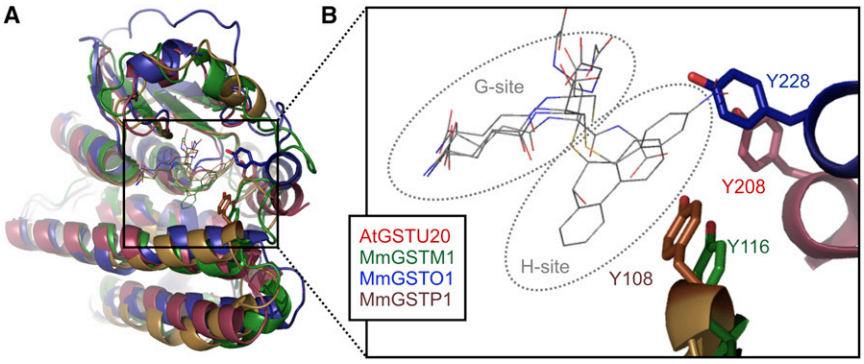

Figure 3. SF Probes Target Tyr Residues at Conserved Positions in Four Different GST Classes

(A) Overlay of the structure of *Mm*GSTP1 with models of structures of *At*GSTU20, *Mm*GSTM1, *Mm*GSTO1, and *Mm*GSTP1.

(B) Close-up of Tyr residues that are targeted by SF probes. All these Tyr residues (right) point with their hydroxyl group into the substrate-binding H-site (middle), which is located next to the glutathione-binding G-site (left). For more details, see Figure S5.

See also Figure S6 and Tables S2–S4.

SjGST Is Labeled at Y111, as Predicted

To investigate whether the labeling site could be predicted for other GSTs, we took advantage of the well-studied *Sj*GST, a GST from the human parasite *Schistosoma japonicum* (McTigue et al., 1995), which has been widely used as a fusion tag for affinity purification of fusion proteins. *Sj*GST is distinctly classified as a helminth GST and is structurally most similar to the GST-Mu class (Sheehan et al., 2001). *Sj*GST is easily expressed in *E. coli*, and more than 14 crystal structures of *Sj*GST have been reported with glutathione and other ligands (Table S5).

We found that *Sj*GST is intensively labeled by DS6R (Figure 4A). Heat treatment blocks DS6R labeling, indicating that the *Sj*GST folding and correct conformation are important for labeling (Figure 4A, lane 2). Preincubation with AEBSF or DS6B suppresses DS6R labeling, illustrating that DS6R targets the same site as AEBSF and DS6B (Figure 4A, lanes 4 and 6). Labeling of *Sj*GST by DS6R reaches a maximum within 10 min and is optimal at pH 7–9 (Figure S7).

*Sj*GST contains 14 tyrosines, of which at least 10 have the hydroxyl group on the surface of GST (Figure 4B). Alignment of the *Sj*GST structure with the other GST structures indicates that the position of Y111 in *Sj*GST is analogous to those of the labeled tyrosines in *At*GSTU20, *Mm*GSTM1, *Mm*GSTO1, and *Mm*GSTP1 (Figure 4C). Y104 is farther away but still in the H-site (Figure 4C). We therefore generated *Sj*GST mutants by substituting the Tyr by a Phe residue, resulting in the Y104F and Y111F mutants of *Sj*GST. Importantly, the Y111F mutant cannot be labeled with DS6R, whereas the Y104F mutant is labeled in a manner similar to labeling for wild-type *Sj*GST (Figure 4D). This experiment demonstrates that Y111 is the only labeling site of *Sj*GST, exactly as predicted by the preceding labeling studies.

Y111 Is Essential for SjGST Activity

The selective labeling of particular Tyr residues in GSTs suggests that either (1) these Tyr residues have no function in GST conjugation, but they react with DS6R because DS6R is trapped in the substrate binding site; or (2) these Tyr residues react with DS6R because they are in an elevated reactive state. We therefore tested whether the Y111 residue has functional relevance in GST function. Mutant *Sj*GST were subjected to different experiments to test their activity. Similar to wild-type *Sj*GST, both Y104F and Y111F *Sj*GST mutants are able to bind glutathione beads, indicating that these mutations do not affect glutathione binding affinity (Figure 5A). Importantly, however, the Y111F mutant is severely hampered in conjugation of glutathione with 7-chloro-4-nitrobenz-2-oxa-1,3-diazole (NBD-Cl), whereas the Y104F mutant has wild-type *Sj*GST activity (Figure 5B). The Y111F substitution yields a 3-fold decrease of the k_{cat} value compared to WT and Y104F proteins, whereas the K_M value increases 5.5-fold (Figure 5C). The catalytic efficiency (k_{cat}/K_M) is 68 mM/s in WT and Y104F mutants, but it is drastically reduced to 3.61 mM/s in the Y111F mutant. This reflects the nonproductive binding of NBD-Cl at the active site in the ternary complex of the Y111F mutant. These data demonstrate that Y111 is essential for the catalytic activity of *Sj*GST toward the NBD-Cl substrate.

DISCUSSION

Using a chemical proteomics approach, we discovered that in addition to targeting serine proteases (Shannon et al., 2012), SF-based probes also specifically target functional tyrosine residues in different classes of GSTs in plant and mouse proteomes. Several previous studies have pointed out that Tyr residues in the H-site play a pivotal role during catalysis, depending on the substrate being tested. Site-directed mutagenesis revealed essential roles for Y212 in human GSTA4-4, Y115 in rat GSTM1-1, Y108 in human GSTP1-1, and Y107 in soybean GSTU4-4 in the conjugation of 4-hydroxynon-2-enal, phenanthrene 9,10-oxide, ethacrynic acid, and fluorodifen, respectively (Bruns et al., 1999; Johnson et al., 1993; Lo Bello et al., 1997; Axarli et al., 2009a). Consistent with these studies, we found that the Y111F *Sj*GST mutant is impaired in conjugating NBD-Cl (Figure 5). Based on crystal structures and enzymatic studies, it is generally believed that the hydroxyl of these Tyr residues donates a hydrogen bond to the substrate to orientate the substrate and enhance its reactivity toward the ionized sulfhydryl of the glutathione residue bound in the nearby G-site (Bruns et al., 1999; Johnson et al., 1993; Lo Bello et al., 1997; Axarli et al., 2009b; Oakley et al., 1997; Quesada-Soriano et al., 2009). That these precise Tyr residues, and not other surface-exposed Tyr residues on GSTs, are labeled with SF-based probes in whole proteomes is fully in line with observations from previous reports on GSTs. This property can be used to study GSTs globally in proteomes.

Our observation that the labeled Tyr residues are functionally relevant suggests that their chemical hyperreactivity (in comparison to the reactivity of other Tyr residues) is caused by an activated state of the hydroxyl group. Such hyperreactivity of

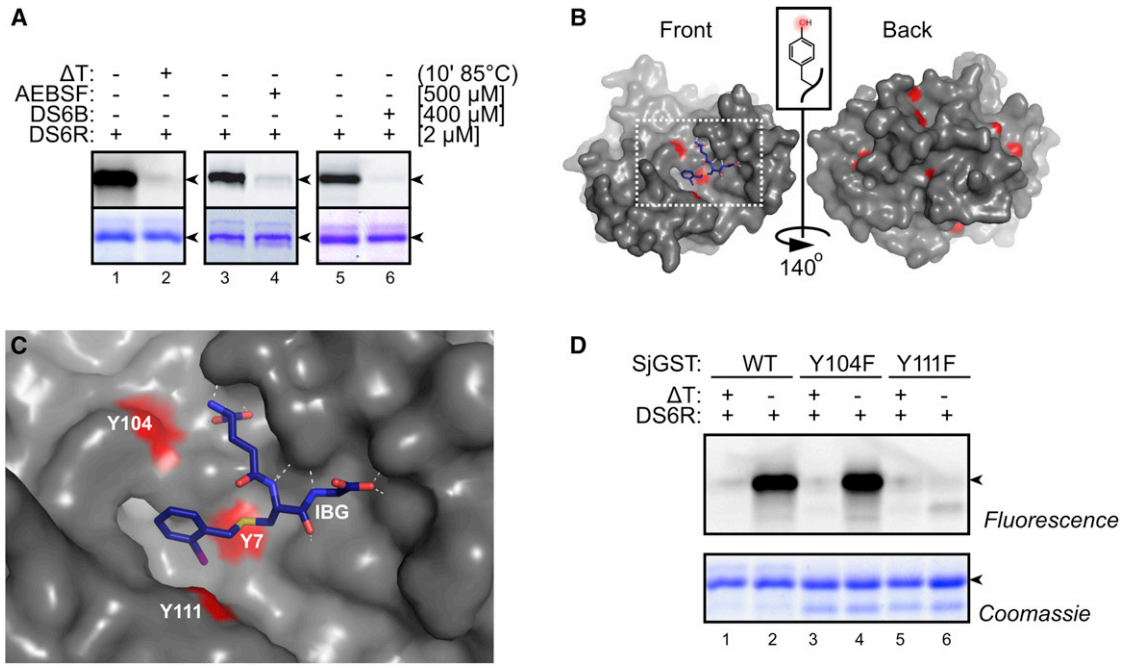

Figure 4. *Sj*GST Is Labeled at Y111, as Predicted

(A) *Sj*GST is labeled by DS6R. Extracts containing *Sj*GST were heated for 10 min at 85°C or preincubated for 15 min with 500 μM AEBSF or 400 μM DS6B and then labeled with 2 μM DS6R for 15 min at pH 8. Proteins were detected from protein gel by fluorescent scanning and Coomassie blue staining.

(B) Crystal structure of *Sj*GST bound to γ-glutamyl[S-(2-iodobenzyl)cysteinyl]glycine (IBG, blue sticks) (1m9b [Cardoso et al., 2003]). The protein surface is shown in gray and the hydroxyl groups of the 14 tyrosines in red.

(C) Enlargement of outlined section in (B) showing the substrate-binding cleft with IBG (blue) and the hydroxyl groups (red) of three tyrosines, Y104, Y111, and the catalytic Y7.

(D) *Sj*GST is labeled at Y111 by DS6R. *E. coli* extracts containing 7.5 μg (mutant) *Sj*GST were treated with or without heating (10 min at 85°C) and labeled with 2 μM DS6R for 15 min at pH 8. Proteins were detected from the protein gel by fluorescent scanning and Coomassie blue staining.

See also Table S5.

Tyr residues is likely to occur if, for example, the local environment enhances deprotonation of the hydroxyl moiety. For instance, it has been suggested that in GmGSTU4-4, a nearby Arg residue enhances the reactivity of the Tyr residue (Axarli et al., 2009b). Deprotonation of the Tyr results in the generation of a phenolate anion that displays an enhanced nucleophilicity toward electrophilic groups such as the fluorosulfonate moiety in SF probes. This theory is supported by the fact that labeling with SF probes decreases at acidic pH when the Tyr is more likely to be in a protonated state.

Although at similar positions in the GST structures, the labeled Tyr is not conserved in the protein sequence. In fact, the four different GST classes share less than 30% sequence homology with each other. The low conservation of the labeled Tyr residues is explained by the promiscuity of the H-sites in GSTs, as these enzymes have to handle a structurally diverse range of small molecules. Our data indicate that chemical proteomics with SF probes has great potential to highlight unconserved, functionally relevant Tyr residues. Structural studies indicate that many other GSTs carry a Tyr at similar positions in the H-site (e.g., Bruns et al., 1999; Johnson et al., 1993; Lo Bello et al., 1997; Axarli et al., 2009b; Oakley et al., 1997; Quesada-Soriano et al., 2009). Consistent with this, we have also detected labeling of GSTF6/11 and GSTU19 from *Arabidopsis* and GSTA3/4, GSTK1, GSTM1/2/3/5/6, GSTO1, and GSTP1 from mouse (Table S2). Thus, we anticipate that SF probes can be used to monitor the availability and reactivity of functional Tyr residues of the majority of GSTs in crude proteomes.

Interestingly, besides the abundant and ubiquitous GSTs, there are dozens of other proteins labeled by SF-based probes (Figure 1; Shannon et al., 2012). Sequences of DAS1-labeled peptides (Table S3) indicate that aldo-keto reductases AKR1A4 and AKR1C6 are labeled by DAS1 on their catalytic Tyr residues (Mindnich and Penning, 2009), whereas protein disulphide isomerase Erp27 and fumarylacetoacetate hydrolase Fah are labeled at a conserved Tyr in the substrate binding site (Bateman et al., 2001; Kober et al., 2013). These data are consistent with the observation that phenylsulfonyl ester probes also label Tyr residues in proteins, but not isolated Tyr amino acids in solution, in contrast to other carbon electrophiles, which do not label Tyr residues (Weerapana et al., 2008). Further studies are required to confirm labeling at these sites as well as the relevance of these Tyr residues. Exploration of additional labeling sites of SF probes will be instrumental to the annotation of functional Tyr residues in proteins.

SIGNIFICANCE

We showed that in addition to serine proteases and many other proteins, sulfonyl fluoride probes also label diverse

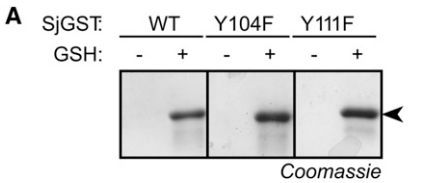

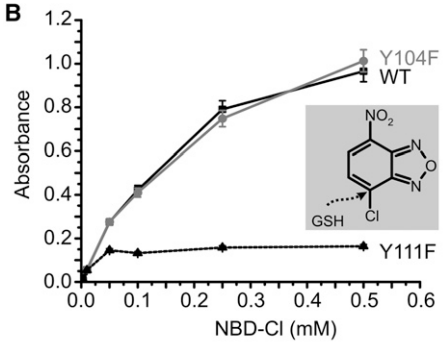

C

SjGST	K_M (mM)	V_{max}	k_{cat} (sec^{-1})
-WT	0.05± 0.002	34.48± 1.72	3.4 ± 0.2
-Y104F	0.05± 0.002	34.48± 1.72	3.4 ± 0.2
-Y111F	0.277± 0.013	10.0± 0.5	1.00 ± 0.05

Figure 5. Y111F Substitution in *Sj*GST Affects NBD-Cl Conjugation but Not Glutathione Binding

(A) Mutant proteins are able to bind glutathione beads. Glutathione beads were incubated with (mutant) *Sj*GST proteins and washed. Proteins were eluted without (−) and with (+) 10 mM glutathione in the elution buffer, and proteins in the eluate were detected on protein gels by Coomassie blue staining.

(B) Y111F mutant is hampered in conjugation of NBD-Cl with glutathione. (Mutant) *Sj*GST proteins were incubated with various NBD-Cl concentrations and the conjugate concentration was determined by measuring the absorbance at 419 nm for 10 min. Error bars indicate the standard deviation of three measurements. The experiment was repeated three times with similar results.

(C) Steady-state catalytic parameters of wild-type and mutant *Sj*GST proteins with NBD-Cl as a substrate. The unit used for V_{max} is μmol/min/mg protein. Values are given as the mean ± SEM for three independent experiments.

GSTs in both plant and mouse proteomes. Importantly, labeling occurs at nonconserved Tyr residues that reside at similar positions in the promiscuous substrate-binding pockets of GSTs representing different subfamilies. These Tyr residues are essential for GST function, possibly because these residues polarize diverse small-molecule substrates to promote conjugation with glutathione. This chemical proteomics study illustrates that SF probes can be used to monitor GSTs in different proteomes and indicates that SF probes highlight functionally relevant Tyr residues in other proteins.

EXPERIMENTAL PROCEDURES

Probes and Probe Synthesis

The synthesis of DS6R and DAS1 has been described elsewhere (Shannon et al., 2012). DS6B was synthesized as follows. Commercially available AEBSF hydrochloride (48 mg, 0.24 mmol) was added to a mixture of Boc-Gly-OH (35 mg, 0.2 mmol), HOBt (37 mg, 0.24 mmol), HBTU (92 mg, 0.24 mmol), and TEA (83 μl, 0.6 mmol) in dichloromethane (1 ml) and stirred for 3 hr. The reaction mixture was subsequently evaporated to dryness, and 50% trifluoroacetic acid in dichloromethane (1 ml) was added to the residue and stirred for 1 hr. After evaporation to dryness, toluene was added (5 ml) and removed again at reduced pressure. A mixture of biotin (59 mg, 2.4 mmol), PyBOP (104 mg, 2.4 mmol), and TEA (110 μl, 0.8 mmol) in DMSO (0.5 ml) were added, and the resulting mixture was stirred overnight. A mixture of ethylacetate/diethyl ether (5 ml, 1:1) was added and the precipitate was isolated and washed first with sodium bicarbonate solution and then with ethyl ether. The residue was dried and purified by preparative reverse-phase high-performance liquid chromatography to yield 43 mg (36%) of DS6B as a white solid. 1H-NMR (DMSO-d6) yielded chemical shifts of δ = 8.04 (d, J = 8.2 Hz, 2H), 7.95 (t, J = 5.48 Hz, 1H), 7.79 (d, J = 8.2 Hz, 1H), 7.68 (t, J = 5.48 Hz, 1H), 7.58 (d, J = 8.2 Hz, 2H), 6.35 (br s, 2H), 4.28 (m, 1H), 4.12 (m, 1H), 3.59 (d, J = 5.84 Hz, 2H), 3.33 (m, 3H), 3.09 (m, 2H), 2.99 (m, 1H), 2.86 (t, J = 6.84 Hz, 2H), 2.78 (dd, J = 12.52, 5.08 Hz, 1H), 2.55 (d, J = 12.52 Hz, 1H), 2.06 (m, 4H), and 1.61–1.26 (m, 11H). The expected ion for electrospray and MS is 600.74 Da ($C_{26}H_{39}FN_5O_6S_2$ $[M^+H]^+$), which corresponds to the found 600.20 Da.

Labeling of Plant Proteomes

Arabidopsis thaliana ecotype Col-0 plants were grown in a light cabinet at 22°C under short-day conditions. Four-week-old plants were used for protein extraction. Proteins were extracted by grinding one rosette leaf in an Eppendorf tube. The extract was mixed with 0.5 ml of water and cleared by centrifugation for 1 min at 16,000 × *g*. Labeling was usually done by incubating 20 μg protein in 0.5 ml total volume containing 50 mM 2-amino-2-hydroxymethyl-1,3-propanediol (TRIS) buffer (pH 8) and 2 μM DS6R for 2 hr at room temperature (22°–25°C) in the dark under gentle agitation. Equal volumes of DMSO were added to the no-probe controls. Proteins were precipitated after labeling by adding 1 ml of ice-cold acetone and subsequent centrifugation for 1 min at 16,000 × *g*. The pellet was dissolved in 2× SDS-PAGE loading buffer containing β-mercaptoethanol, and separated on 12% SDS gels (8 μg protein per lane). Labeled proteins were visualized by in-gel fluorescence scanning using a Typhoon 8600 scanner (GE Healthcare Life Sciences, http://www.gelifesciences.com/) with excitation and emission at 532 and 580 nm, respectively. Fluorescent signals were quantified with ImageQuant 5.2 (GE Healthcare Life Sciences). Alternatively, protein extracts were labeled with 2 μM DS6B. After SDS PAGE, proteins were transferred onto polyvinylidene fluoride membrane (Immobilon-P; Millipore, http://www.millipore.com/) and detected using streptavidin-horseradish peroxidase (1:3000; Ultrasensitive, Sigma, http://www.sigmaaldrich.com/). Profiling at various pH values was done using 50 mM sodium acetate (pH 4–6.5) and Tris (pH 7–11) buffers, or 50 mM phosphate buffer (pH 4–11).

Affinity Purification and Identification of Labeled Plant Proteins

Proteins of 8-week-old *Arabidopsis* plants were extracted by grinding rosette leaves of 30 plants in an ice-cold mortar with 10 ml water and subsequent centrifugation for 10 min at 20,000 × *g*. Five milliliters of supernatant at 4 mg/ml was labeled with 20 μM DS6B in 50 mM TRIS buffer (pH 10) for 3 hr at room temperature under gentle agitation. The labeled leaf extracts were applied to PD-10 size-exclusion columns (Bio-Rad, http://www.bio-rad.com/) to remove unlabeled probe. Desalted samples were incubated with 100 μl of streptavidin agarose beads (Pierce, http://www.piercenet.com/) for 1.5 hr at room temperature under gentle agitation. Streptavidin agarose beads were collected by centrifuging for 10 min at 3,000 × *g* and washed twice with 0.1% SDS, twice with 6 M urea, once with 50 mM TRIS (pH 8) containing 1% Triton X-100, once with 1% Triton X-100, and once with water, then boiled in 30 μl of 2× SDS-PAGE loading buffer containing b-mercaptoethanol. Affinity-purified proteins were separated on 12% one-dimensional SDS gel and stained with Coomassie blue (Imperial Protein Stain, Pierce). The specific band was excised from the Coomassie-blue-stained gel and subjected to in-gel tryptic digestion and subsequent MS analysis.

Protein Digestion and Analysis by MALDI MS/MS

Bands were visually selected from Coomassie-blue-stained gels, robotically excised, and digested with trypsin using the Proteineer spII and dp systems (Bruker Daltonics), and spotted robotically onto Anchorchip steel targets (Bruker) with a thin layer of α-cyano-4-hydroxycinnamic acid matrix (Gobom et al., 2001). Peptide mass fingerprint data were collected on an UltraflexIII MALDI TOF/TOF mass spectrometer (Bruker) and used for a first round of database searching using MASCOT 2.3 (http://www.matrixscience.com)

against the TAIR10 database of *Arabidopsis* proteins (http://www.arabidopsis.org). Searches allowed a single miscleavage by trypsin and a DS6B modification on hydrophilic residues (CDEHKMNQRSTY). Because the one-dimensional gel band in question contained a mixture of GSTs, the peptide mass fingerprint searches failed to identify proteins. This sample was used to select precursors for subsequent MS/MS analysis. Following sample recrystallization, LIFT MS/MS spectra were collected for 11 suitable precursors (Suckau et al., 2003), and these data were used to search TAIR10, allowing for a DS6B modification on any polar amino acid. The resulting search found two unmodified peptides belonging to *At*GSTU20 and one modified peptide that fell well below the Mascot 95% significance threshold but above the best decoy peptide. A more detailed visual inspection of this peptide spectrum revealed additional assignable ions, verifying the presence of the modification and pinpointing the modified tyrosine residue in the sequence (see Figures 2 and S1).

Labeling, Affinity Purification, and Identification of DAS1-Labeled Mouse Proteomes

For protein labeling and click chemistry, proteome samples were diluted to a 2 mg protein/ml solution in PBS. Each sample (4 × 0.5 ml aliquots) was treated with 100 μM of probe (from a stock in DMSO). The labeling reactions were incubated at room temperature for 1 hr. Click chemistry was performed by the addition of 100 μM of the TEV-biotin tag (50× stock in DMSO [Weerapana et al., 2007, 2010]), 1 mM TCEP (fresh 50× stock in water), 100 μM ligand (17× stock in DMSO:t-butanol 1:4) and 1 mM $CuSO_4$ (50× stock in water). Samples were allowed to react at room temperature for 1 hr. Tubes were combined pairwise and centrifuged (5,900 × *g* for 4 min at 4°C) to pellet the precipitated proteins. The pellets were resuspended in cold MeOH by sonication and tubes were combined pairwise. Centrifugation was followed by a second methanol wash, after which the pellet was solubilized via sonication in PBS containing 1.2% SDS and incubated at room temperature for 5 min. The SDS-solubilized, probe-labeled proteome samples were diluted with 5 ml of PBS for a final SDS concentration of 0.2%. The solutions were then incubated with 100 μl of streptavidin-agarose beads (Pierce) for 15 hr at 4°C and for an additional 3 hr at room temperature. The beads were washed with 5 ml 0.2% SDS/PBS, then three times with 5 ml PBS and three times with 5 ml H_2O, and the beads were pelleted by centrifugation (1,300 × *g* for 2 min) between washes. The washed beads were suspended in 500 μl of 6 M urea/PBS and 10 mM DTT (from 20× stock in H_2O) and allowed to react for 15 min at 65°C. Then 20 mM iodoacetamide (from 50× stock in H_2O) was added and allowed to react at 37°C for 30 min. Following reduction and alkylation, the beads were pelleted by centrifugation (1,300 × *g* for 2 min) and resuspended in 150 μl of 2 M urea/PBS, 1 mM $CaCl_2$ (100× stock in H2O), and trypsin (2 μg). The digestion was allowed to proceed overnight at 37°C with mild agitation. The digest was separated from the beads using a Micro Bio-Spin column and the beads were then washed three times with 500 μl PBS, three times with 500 μl H_2O, and once with 150 μl of TEV digest buffer. The washed beads were then resuspended in 150 μl of TEV digest buffer with AcTEV Protease (5 μl; Invitrogen) for 12 hr at 29°C with mild agitation. The eluted peptides were separated from the beads using a Micro Bio-Spin column and the beads were washed twice with 75 μl H_2O. Formic acid (15 μl) was added to the sample, which was stored at −20°C until mass spectrometry analysis.

DAS1-labeled samples were analyzed by liquid chromatography-MS on an LTQ Orbitrap Discovery mass spectrometer (ThermoFisher) coupled to an Agilent 1200 series HPLC. TEV digests were pressure loaded onto a 250 μm fused silica desalting column packed with 4 cm of Aqua C18 reverse phase resin (Phenomenex). The peptides were then eluted onto a biphasic column (100 μm fused silica) with a 5 μm tip, packed with 10 cm C18 and 3 cm Partisphere strong cation exchange resin (Whatman) using a gradient of 5%–100% Buffer B in Buffer A (Buffer A: 95% water, 5% acetonitrile, and 0.1% formic acid; Buffer B: 20% water, 80% acetonitrile, and 0.1% formic acid). The peptides were then eluted from the strong cation exchange resin onto the C18 resin and into the mass spectrometer using four salt steps as outlined previously (Speers and Cravatt, 2005; Weerapana et al., 2007). The flow rate through the column was set to ~0.25 μl/min and the spray voltage was set to 2.75 kV. One full MS scan in the Orbitrap (400–1,800 MW, 30,000 resolution) was followed by 18 data-dependent scans in the ion trap of the nth most intense ions with dynamic exclusion disabled.

The generated tandem-MS data were searched using the SEQUEST algorithm against version 3.23 of the mouse IPI database. A static modification of +57 on Cys was specified to account for iodoacetamide alkylation. For the probe-labeled samples, a differential modification of +667.3145 (mass corresponding to use of the Heavy TEV-biotin tag [Weerapana et al., 2010]) was specified on Cys, Lys, Ser, Thr, and Tyr. SEQUEST output files were filtered using DTASelect 2.0 with default parameters that specified a target-peptide false-positive rate of 5%. Reported peptides were also required to be fully tryptic and contain the desired probe modification. Data sets were obtained for soluble mouse liver proteome (three data sets) and soluble mouse pancreas proteome (one data set). These data were collated into an Excel file format, and further analysis was performed to screen for peptides that appeared in two or more data sets with two or more spectral counts in each data set. Peptides that contained two or more missed tryptic cleavage sites within the peptide were removed. For peptides that appeared as labeled at more than one amino acid within the peptide sequence, manual sequencing was performed to verify that labeling occurred at the indicated tyrosine residue.

SjGST Mutagenesis, Labeling, and Activity Assays

*Sj*GST mutants were generated by Quick Change site-directed mutagenesis (Stratagene) using primers 5′-gttttggatattagattcggtgtttcgag-3′ and 5′-ctcg aaacaccgaatctaatatccaaac-3′ for *Sj*GST-Y104F and 5′-cgagaattgcatttagtaaa gacttg-3′ and 5′-caagtctttactaaatgcaattctcg-3′ for *Sj*GST-Y111F with pGEX-4T1 (GE Healthcare) as a template. Plasmids were verified by sequencing and transformed into BL21 (DE3) cells. Proteins were expressed by growing a 10 ml culture in LB medium containing 100 mg/l ampicillin until OD_{600nm} = 0.6–1.0 and inducing with 0.8 mM isopropyl β-D-1-thiogalactopyranoside for 12 hr at 37°C. Cells were lysed by sonification and centrifuged for 30 min at 6000 × *g*. Proteins were precipitated from the supernatant in 95% ammonium sulfate and the pellet was dissolved in 1 ml binding buffer (50 mM Tris-HCl [pH 8]). The samples were incubated for 60 min. with 50 μl glutathione-sepharose 4B matrix (GE Healthcare), equilibrated with binding buffer. The matrix was washed three times with binding buffer and eluted with binding buffer containing 10 mM glutathione.

For labeling assays, *E. coli* were cultured in 5 ml of LB medium containing 100 mg/l ampicillin at 37°C until OD600 = 0.6–0.8 and then induced with 1 mM isopropyl β-D-1-thiogalactopyranoside for 12 hr at 37°C. Cells were lysed by sonification and centrifuged for 1 min at 16,000 × *g*. Heat treatment was done by incubating protein extracts at 85°C for 10 min in a heating block and then chilling on ice. Labeling was usually done by incubating 5 μg protein in 50 μl total volume containing 50 mM Tris buffer (pH 8) and 2 μM DS6R for 15 min at room temperature in the dark under gentle agitation. Competition assays were done by preincubating the protein extracts with inhibitor or competitor molecules (e.g., 500 μM AEBSF or 400 μM DS6B) for 15 min before DS6R labeling. Labeling reaction was terminated by adding 10 μl of 6× SDS-PAGE loading buffer containing b-mercaptoethanol and heating at 95°C for 5 min, after which the labeled proteins were separated on 12% SDS gels (1.5 μg protein per lane). Fluorescence visualization and quantification were carried out as described above. GST activity assays were performed in 200 μl total volume containing 1.8–2.4 μg *Sj*GST proteins in the presence of 100 mM sodium acetate (pH 5) and 2 mM glutathione and 0.0025–1 mM NBD-Cl (SantaCruz). Absorbance was detected every minute for 20 min at 419 nm using the Synergy-4 plate reader (Biotek).

SUPPLEMENTAL INFORMATION

Supplemental Information includes seven figures and five tables and can be found with this article online at http://dx.doi.org/10.1016/j.chembiol.2013.01.016.

ACKNOWLEDGMENTS

We thank Réka Tóth for useful comments and critical reading, and Jieung Shin for providing materials. This work has been supported by the Max Planck Society, the Deutsche Forschungsgemeinshaft (DFG projects HO3983/4-1, SCH2476/2-1, and KA2894/1-1), NIH CA087660 ERC Starting Grant no. 258413, the Humboldt Foundation, the Smith Family Foundation and Boston College, and COST Action CM 1004.

Received: October 10, 2012
Revised: January 7, 2013
Accepted: January 12, 2013
Published: April 18, 2013

REFERENCES

Arnold, K., Bordoli, L., Kopp, J., and Schwede, T. (2006). The SWISS-MODEL workspace: a web-based environment for protein structure homology modelling. Bioinformatics *22*, 195–201.

Axarli, I., Dhavala, P., Papageorgiou, A.C., and Labrou, N.E. (2009a). Crystal structure of Glycine max glutathione transferase in complex with glutathione: investigation of the mechanism operating by the Tau class glutathione transferases. Biochem. J. *422*, 247–256.

Axarli, I., Dhavala, P., Papageorgiou, A.C., and Labrou, N.E. (2009b). Crystallographic and functional characterization of the fluorodifen-inducible glutathione transferase from Glycine max reveals an active site topography suited for diphenylether herbicides and a novel L-site. J. Mol. Biol. *385*, 984–1002.

Bateman, R.L., Bhanumoorthy, P., Witte, J.F., McClard, R.W., Grompe, M., and Timm, D.E. (2001). Mechanistic inferences from the crystal structure of fumarylacetoacetate hydrolase with a bound phosphorus-based inhibitor. J. Biol. Chem. *276*, 15284–15291.

Board, P.G., Coggan, M., Chelvanayagam, G., Easteal, S., Jermiin, L.S., Schulte, G.K., Danley, D.E., Hoth, L.R., Griffor, M.C., Kamath, A.V., et al. (2000). Identification, characterization, and crystal structure of the Omega class glutathione transferases. J. Biol. Chem. *275*, 24798–24806.

Bruns, C.M., Hubatsch, I., Ridderström, M., Mannervik, B., and Tainer, J.A. (1999). Human glutathione transferase A4-4 crystal structures and mutagenesis reveal the basis of high catalytic efficiency with toxic lipid peroxidation products. J. Mol. Biol. *288*, 427–439.

Cardoso, R.M.F., Daniels, D.S., Bruns, C.M., and Tainer, J.A. (2003). Characterization of the electrophile binding site and substrate binding mode of the 26-kDa glutathione S-transferase from Schistosoma japonicum. Proteins *51*, 137–146.

Cravatt, B.F., Wright, A.T., and Kozarich, J.W. (2008). Activity-based protein profiling: from enzyme chemistry to proteomic chemistry. Annu. Rev. Biochem. *77*, 383–414.

Dixon, D.P., and Edwards, R. (2010). Glutathione transferases. Arabidopsis Book *8*, e0131.

Edwards, R., Dixon, D.P., and Walbot, V. (2000). Plant glutathione S-transferases: enzymes with multiple functions in sickness and in health. Trends Plant Sci. *5*, 193–198.

Gobom, J., Schuerenberg, M., Mueller, M., Theiss, D., Lehrach, H., and Nordhoff, E. (2001). Alpha-cyano-4-hydroxycinnamic acid affinity sample preparation. A protocol for MALDI-MS peptide analysis in proteomics. Anal. Chem. *73*, 434–438.

Hayes, J.D., Flanagan, J.U., and Jowsey, I.R. (2005). Glutathione transferases. Annu. Rev. Pharmacol. Toxicol. *45*, 51–88.

Heal, W.P., and Tate, E.W. (2010). Getting a chemical handle on protein post-translational modification. Org. Biomol. Chem. *8*, 731–738.

Jeffery, D.A., and Bogyo, M. (2003). Chemical proteomics and its application to drug discovery. Curr. Opin. Biotechnol. *14*, 87–95.

Johnson, W.W., Liu, S., Ji, X., Gilliland, G.L., and Armstrong, R.N. (1993). Tyrosine 115 participates both in chemical and physical steps of the catalytic mechanism of a glutathione S-transferase. J. Biol. Chem. *268*, 11508–11511.

Kober, F.X., Koelmel, W., Kuper, J., Drechsler, J., Mais, C., Hermanns, H.M., and Schindelin, H. (2013). The crystal structure of the protein disulfide isomerase family member ERp27 provides insights into its substrate-binding capabilities. J. Biol. Chem. *288*, 2029–2039.

Lo Bello, M., Oakley, A.J., Battistoni, A., Mazzetti, A.P., Nuccetelli, M., Mazzarese, G., Rossjohn, J., Parker, M.W., and Ricci, G. (1997). Multifunctional role of Tyr 108 in the catalytic mechanism of human glutathione transferase P1-1. Crystallographic and kinetic studies on the Y108F mutant enzyme. Biochemistry *36*, 6207–6217.

McTigue, M.A., Williams, D.R., and Tainer, J.A. (1995). Crystal structures of a schistosomal drug and vaccine target: glutathione S-transferase from *Schistosoma japonica* and its complex with the leading antischistosomal drug praziquantel. J. Mol. Biol. *246*, 21–27.

Mindnich, R.D., and Penning, T.M. (2009). Aldo-keto reductase (AKR) superfamily: genomics and annotation. Hum. Genomics *3*, 362–370.

Oakley, A.J., Lo Bello, M., Battistoni, A., Ricci, G., Rossjohn, J., Villar, H.O., and Parker, M.W. (1997). The structures of human glutathione transferase P1-1 in complex with glutathione and various inhibitors at high resolution. J. Mol. Biol. *274*, 84–100.

Quesada-Soriano, I., Parker, L.J., Primavera, A., Casas-Solvas, J.M., Vargas-Berenguel, A., Barón, C., Morton, C.J., Mazzetti, A.P., Lo Bello, M., Parker, M.W., and García-Fuentes, L. (2009). Influence of the H-site residue 108 on human glutathione transferase P1-1 ligand binding: structure-thermodynamic relationships and thermal stability. Protein Sci. *18*, 2454–2470.

Rix, U., and Superti-Furga, G. (2009). Target profiling of small molecules by chemical proteomics. Nat. Chem. Biol. *5*, 616–624.

Serim, S., Haedke, U., and Verhelst, S.H.L. (2012). Activity-based probes for the study of proteases: recent advances and developments. ChemMedChem *7*, 1146–1159.

Shannon, D.A., Gu, C., McLaughlin, C.J., Kaiser, M., van der Hoorn, R.A.L., and Weerapana, E. (2012). Sulfonyl fluoride analogues as activity-based probes for serine proteases. ChemBioChem *13*, 2327–2330.

Sheehan, D., Meade, G., Foley, V.M., and Dowd, C.A. (2001). Structure, function and evolution of glutathione transferases: implications for classification of non-mammalian members of an ancient enzyme superfamily. Biochem. J. *360*, 1–16.

Speers, A.E., and Cravatt, B.F. (2005). A tandem orthogonal proteolysis strategy for high-content chemical proteomics. J. Am. Chem. Soc. *127*, 10018–10019.

Suckau, D., Resemann, A., Schuerenberg, M., Hufnagel, P., Franzen, J., and Holle, A. (2003). A novel MALDI LIFT-TOF/TOF mass spectrometer for proteomics. Anal. Bioanal. Chem. *376*, 952–965.

Townsend, D.M., and Tew, K.D. (2003). The role of glutathione-S-transferase in anti-cancer drug resistance. Oncogene *22*, 7369–7375.

Vega, M.C., Walsh, S.B., Mantle, T.J., and Coll, M. (1998). The three-dimensional structure of Cys-47-modified mouse liver glutathione S-transferase P1-1. Carboxymethylation dramatically decreases the affinity for glutathione and is associated with a loss of electron density in the αB-310B region. J. Biol. Chem. *273*, 2844–2850.

Weerapana, E., Speers, A.E., and Cravatt, B.F. (2007). Tandem orthogonal proteolysis-activity-based protein profiling (TOP-ABPP)—a general method for mapping sites of probe modification in proteomes. Nat. Protoc. *2*, 1414–1425.

Weerapana, E., Simon, G.M., and Cravatt, B.F. (2008). Disparate proteome reactivity profiles of carbon electrophiles. Nat. Chem. Biol. *4*, 405–407.

Weerapana, E., Wang, C., Simon, G.M., Richter, F., Khare, S., Dillon, M.B., Bachovchin, D.A., Mowen, K., Baker, D., and Cravatt, B.F. (2010). Quantitative reactivity profiling predicts functional cysteines in proteomes. Nature *468*, 790–795.

Xiao, G., Liu, S., Ji, X., Johnson, W.W., Chen, J., Parsons, J.F., Stevens, W.J., Gilliland, G.L., and Armstrong, R.N. (1996). First-sphere and second-sphere electrostatic effects in the active site of a class mu gluthathione transferase. Biochemistry *35*, 4753–4765.

Yan, X., Luo, Y., Zhang, Z., Li, Z., Luo, Q., Yang, L., Zhang, B., Chen, H., Bai, P., and Wang, Q. (2012). Europium-labeled activity-based probe through click chemistry: absolute serine protease quantification using ^{153}Eu isotope dilution ICP/MS. Angew. Chem. Int. Ed. Engl. *51*, 3358–3363.

